Available online at www.sciencedirect.com
SCIENCE DIRECT
Trans. Nonferrous Met. Soc. China 16(2006) 1171−1177
Transactions of Nonferrous Metals Society of China
www.csu.edu.cn/ysxb/

Corrosion behavior of 2195 and 1420 Al-Li alloys in neutral 3.5% NaCl solution under tensile stress

LI Jin-feng(李劲风), CHEN Wen-jing(陈文敬),
ZHAO Xu-shan(赵旭山), REN Wen-da(任文达) , ZHENG Zi-qiao(郑子樵)

School of Materials Science and Engineering, Central South University, Changsha 410083, China

Received 24 November 2005; accepted 3 March 2006

Abstract: The corrosion behaviors of 1420 and 2195 Al-Li alloys under 308 and 490 MPa tensile stress respectively in neutral 3.5% NaCl solution were investigated using electrochemical impedance spectroscopy(EIS) and scanning electron microscope(SEM). It is found that the unstressed 1420 alloy is featured with large and discrete pits, while general corrosion and localized corrosion including intergranular corrosion and pitting corrosion occur on the unstressed 2195 alloy. As stress is applied to 1420 alloy, the pit becomes denser and its size is decreased. While, for the stressed 2195 alloy, intergranular corrosion is greatly aggravated and severe general corrosion is developed from connected pits. The EIS analysis shows that more severe general corrosion and localized corrosion occur on the stressed 2195 Al-Li alloy than on 1420 Al-Li alloy. It is suggested that tensile stress has greater effect on the corrosion of 2195 Al-Li alloy than on 1420 Al-Li alloy.

Key words: 1420 Al-Li alloy; 2195 Al-Li alloys; corrosion; tensile stress

1 Introduction

Al-Li alloys, compared with traditional Al alloys, possess many excellent properties, such as lower density, greater elastic modulus and higher specific strength. 2195 Al-Li alloy with high strength and good ability to weld, was applied to space shuttle[1]. 1420 Al-Li alloy was developed in Russia and applied to airplane structural components. While, in moist environments, corrosion will occur on Al-Li alloys and deteriorate their mechanical properties. A lot of research work has been done on the corrosion behaviors of unstressed Al-Li alloys. However, stress always exists in Al-Li alloys as they are used. So investigating their corrosion behaviors under tensile stress is very important to their applications.

It has been confirmed that a tensile stress accelerates the corrosion of metals. Tensile stress lowers the break-down potential of 2024-T3 Al alloy and increases its intergranular corrosion penetration rate[2]. LI et al[3] found that tensile stress greatly increased the exfoliation corrosion of a 7075 Al alloy with two-step over-aging, which is not susceptible to exfoliation under conditions of free stress.

Electrochemical Impedance Spectroscopy (EIS) is an efficient method to study electrochemical corrosion. It has been used to study the corrosion of Al and Al alloys in NaCl solution, EXCO solution and thin electrolyte layer[4−6]. A quantitative determination of the exfoliation corrosion of Al alloys is also developed through EIS[7, 8]. BONORA et al[9] studied the corrosion behavior of stressed magnesium alloys using EIS and the results showed that the EIS measurement is a suitable and efficient experimental method to show mechanochemical effects.

In this study, the electrochemical impedance spectroscopy(EIS) of stressed 2195 and 1420 Al-Li alloys in NaCl solution was investigated, and their corrosion morphologies were observed with a scanning electron microscope(SEM).

2 Experimental

The plates of 1420 Al-Li alloy with a thickness of 1.0 mm and 2195 Al-Li alloy with a thickness of 2.0 mm were manufactured by Southwest Aluminum (Group) Co Ltd. Their chemical composition and heat treatment

Foundation item: Project(50401012) supported by the National Natural Science Foundation of China
Corresponding author: LI Jin-feng; Tel: +86-731-8830270; E-mail: lijinfeng@mail.csu.edu.cn

routine are listed in Tables 1 and 2, respectively.

Table 1 Chemical composition of two tested Al-Li alloys (mass fraction, %)

Alloy	Cu	Mg	Li	Ag	Zr	Al
1420	–	5.2	2.0	–	0.11	Bal.
2195	4.0	0.4	1.0	0.4	0.14	Bal.

Table 2 Heat treatment process of two tested Al-Li alloys

Alloy	Treatment process
Peak-aged 1420 Al-Li alloy	Solution treatment at 450 ℃ for 30 min, quenched in water, then aged at 170 ℃ for 16 h
Peak-aged 2195 Al-Li alloy	Solution treatment at 504 ℃ for 30 min, quenched in water, then aged at 170 ℃ for 32 h

Specimens were cut from the aged Al-Li alloy plates according to HB5254—83, of which stressed part has a width of 3−4 mm and length of 65 mm. Their surfaces were ground with abrasive papers and polished with Cr_2O_3 powders. An area of 45 mm^2 on the surface of a specimen was exposed, while the other part was sealed with paraffin. An electrochemical cell was fixed to the specimen, which was clamped to a SCC test machine with a constant stress, as shown schematically in Fig.1. The corrosion medium was 3.5 % NaCl solution at pH=6.5 prepared using analytical NaCl and distilled water.

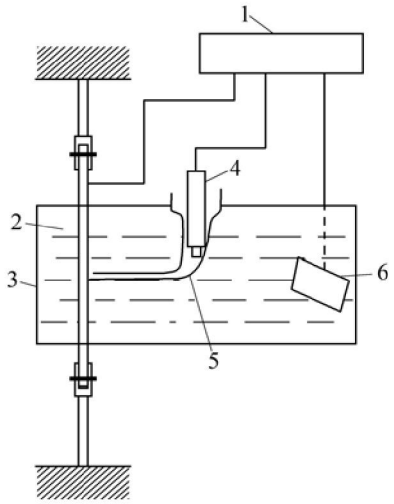

Fig.1 Schematic view of experimental apparatus: 1 SI 1287 solartron electrochemical interface; 2 Specimen (working electrode); 3 Electrochemical cell; 4 Reference electrode(SCE); 5 Luggin capillary; 6 Platinum electrode

The stresses applied to 1420 and 2195 Al-Li alloys were 308 MPa and 490 MPa respectively, which were close to their corresponding yield strengths. As the stress was applied to the alloys, the prepared corrosion medium was poured into the electrochemical cell. During the immersion time, the electrochemical impedance spectroscopy(EIS) measurements were carried out using a three compartment cell. The peak-aged Al-Li alloy was used as a working electrode. A large platinum sheet and a saturated calomel electrode(SCE) with a Luggin capillary served as the counter and the reference electrodes, respectively. The EIS measurement was performed with a SI 1287 Electrochemical Interface at the corrosion potential and always carried out from a high frequency of 1×10^5 Hz to a low frequency of 1 Hz. Then, the EIS data were analyzed with a Zview program.

Meanwhile, some stressed specimens were immersed in the NaCl solution for various days. After immersion, the attacked part was cut from the specimen. The corrosion product on its surface was removed by 2% CrO_3+5% H_3PO_4 solution at 80 ℃ and the corrosion morphologies were observed with a KYKY 2800 SEM.

3 Experiment results

3.1 Electrochemical performance

Fig.2 shows the EIS plot of the stressed 1420 Al-Li alloy immersed in NaCl solution for 16 h. It is clear that this EIS plot is composed of a capacitive arc. As immersion time is increased, two capacitive arcs appear, indicating that localized corrosion occurs. These two capacitive arcs overlap and can not be distinguished in the Nyquist plot (Fig.3(a)). However, they still can be distinguished in the Bode plot, as seen in Fig.3(b).

At the initial stage of immersion, the EIS plot of the stressed 2195 Al-Li alloy comprises a capacitive arc, which is similar to that of the stressed 1420 Al-Li alloy, as shown in Fig.4. Two capacitive arcs appear in the EIS as immersion time increases, which can be distinguished in the Bode plot, as seen in Fig.5.

3.2 Corrosion morphologies

Fig.6 presents the corrosion morphologies of the unstressed and stressed 1420 Al-Li alloys immersed for 9 d. The corrosion morphology of the unstressed alloy is featured with large and discrete pits. As stress is applied, the pits become denser and their size is decreased. Meanwhile, some cracks can be observed. It is also found that slight general corrosion occurs on the unstressed and stressed 1420 Al-Li alloys.

Fig.7 shows the corrosion morphologies of the unstressed and stressed 2195 Al-Li alloys immersed for 3 d. It can be found that general corrosion occurs on the unstressed 2195 alloy surface. Meanwhile, intergranular corrosion(IGC) is a main kind of localized corrosion, and pitting corrosion is also observed, as shown in Fig.7(a). Similarly, for the stressed 2195 alloy, general corrosion and intergranular corrosion appear on the alloy surface.

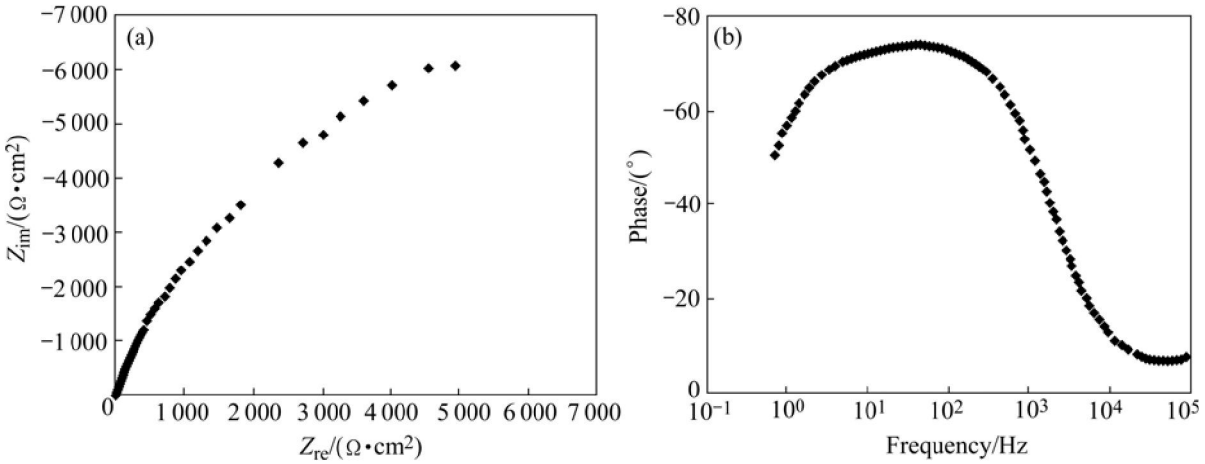

Fig.2 Nyquist (a) and Bode (b) plots of stressed 1420 Al-Li alloy immersed in NaCl solution for 16 h

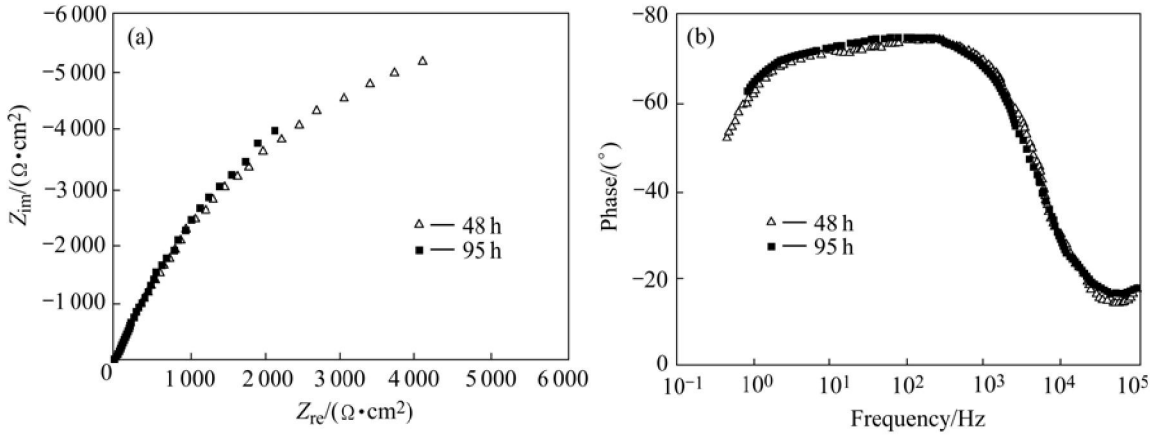

Fig.3 Nyquist (a) and Bode (b) plots of stressed 1420 Al-Li alloy immersed in NaCl solution for 48 h and 95 h

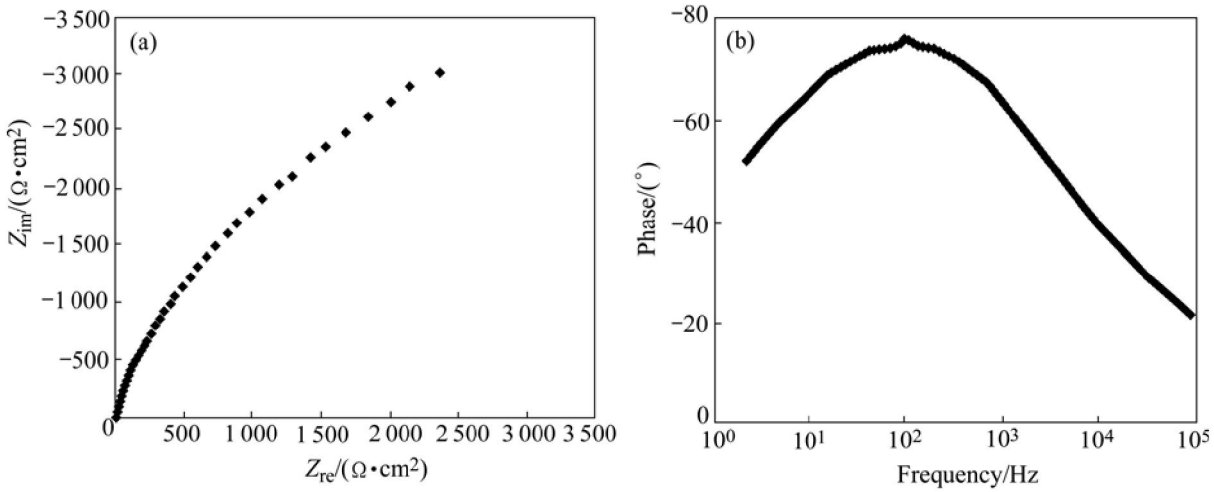

Fig.4 Nyquist (a) and Bode (b) plots of stressed 2195 Al-Li alloy immersed in NaCl solution for 17 h

The general corrosion is developed from multitudinous pits, as shown in Fig.7(b). The intergranular corrosion causes severe corrosion, which penetrates to inside of the alloy (seen in Fig.7(b)).

As immersion time is increased, the pitting corrosion and intergranular corrosion of the unstressed 2195 Al-Li alloy are aggravated, as shown in Fig.8(a). Compared with that of the unstressed and stressed 2195 alloy immersed for 9 d and 3 d respectively, the intergranular corrosion of the stressed 2195 alloy

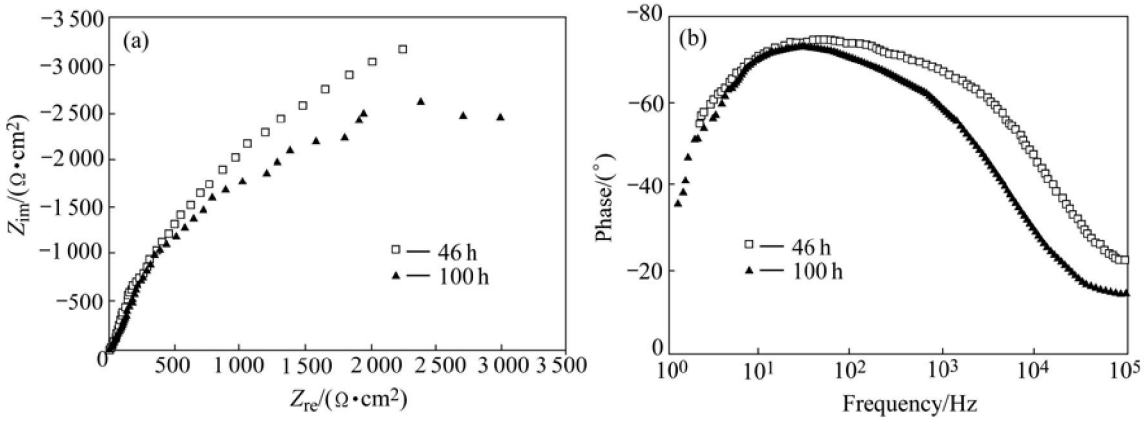

Fig.5 Nyquist (a) and bode (b) plot of stressed 2195 Al-Li alloy immersed in NaCl solution for 46 h and 100 h

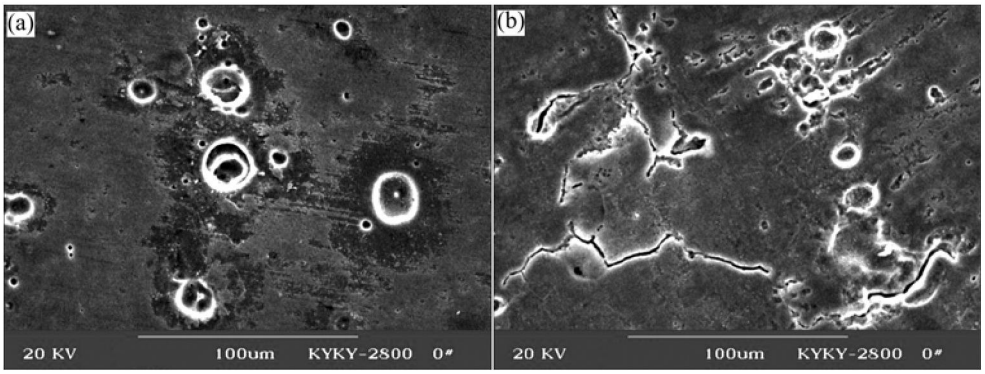

Fig.6 Representative corrosion morphologies of unstressed (a) and stressed (b) 1420 Al-Li alloys immersed for 9 d

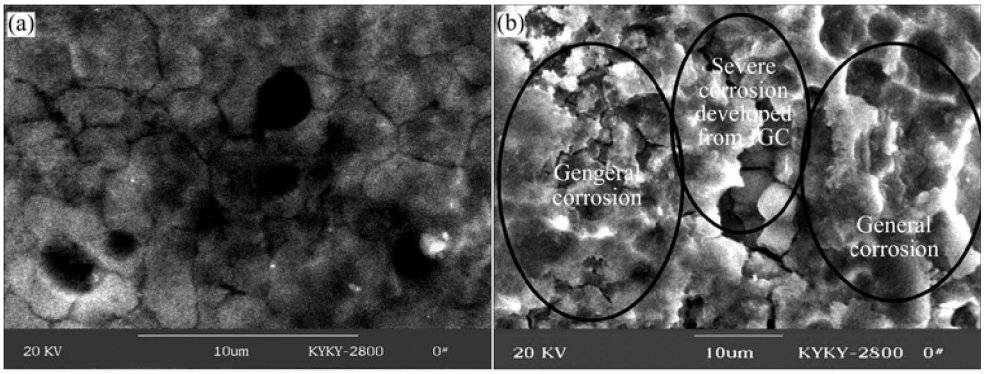

Fig.7 Representative corrosion morphologies of unstressed (a) and stressed (b) 2195 Al-Li alloy immersed for 3 d

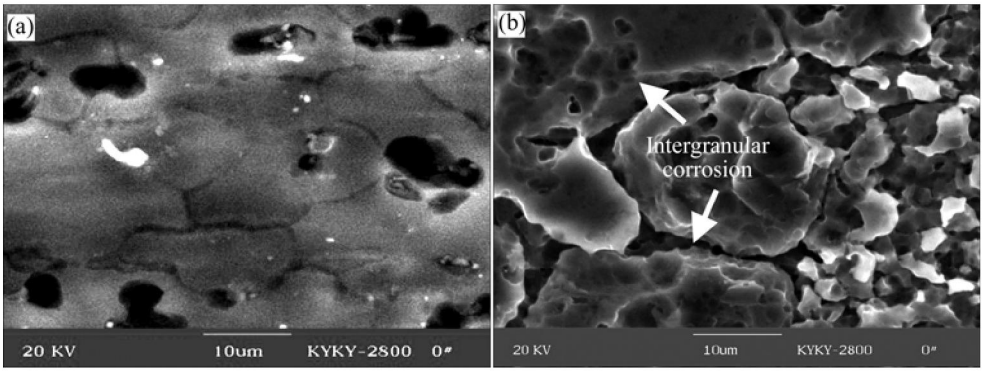

Fig.8 Representative corrosion morphologies of unstressed (a) and stressed (b) 2195 Al-Li alloy immersed for 9 d

immersed for 9 d is greatly increased, and a large number of pits are connected to each other, as seen in Fig.8(b).

From the corrosion morphology observation, it can be found that the unstressed 1420 Al-Li alloy is featured with pitting corrosion. Stress increases the pit density and decreases its size. For the unstressed 2195 Al-Li alloy, general corrosion, intergranular corrosion and pitting corrosion occur. As stress is applied, the intergranular corrosion is greatly aggravated, and severe general corrosion is developed from multi-tudinous pits. Stress has a greater effect on the corrosion behavior of 2195 Al-Li alloy than on that of 1420 Al-Li alloy.

4 Discussion

4.1 Evaluation of corrosion morphology

1420 and 2195 Al-Li alloys are age strengthened alloys. Two main precipitates of 2195 alloy are T_1 (Al_2CuLi) and θ'(Al_2Cu), which appear at dislocations, subgrain and grain boundaries. Meanwhile, equivalent phase T_2 (Al_6CuLi_3) precipitates along grain boundaries. During the precipitation of θ', T_1 and T_2, a Cu and Li-depleted precipitate-free zone(PFZ) is formed along grain boundaries and subgrain boundaries, due to the absorption of Cu and Li atoms to T_1, T_2 and θ' phase [10−12]. The main precipitate of 1420 alloy is δ'(Al_3Li), which is coherent to the alloy base and precipitates evenly. While, another possible precipitate in Al-Mg-Li alloy is S'(Al_2MgLi) [13]. In studied 2195 Al-Li alloy, it is found that T_1 precipitates within the grains, and coarse equivalent T_2 exists at the grain boundaries, as seen in Fig.9(a). While, in 1420 alloy aged at 170℃ for 16 h, δ' precipitates evenly within the grains (seen in Fig.9(b)) and little S' precipitates along grain boundaries (seen in Fig.9(c)).

The difference of the corrosion morphology of the unstressed 1420 Al-Li alloy with the unstressed 2195 Al-Li alloy should be associated with the precipitates and their distribution. The main precipitate of δ' in 1420 alloy is anodic to the alloy base. However, it distributes uniformly in the alloy, and little equivalent phase Al_2Mg-Li precipitates along the grain boundaries. As a result, electrochemical driving force for intergranular corrosion does not exist, and only pitting corrosion occurs.

LI et al[14] studied the function mechanism of T_1 in the localized corrosion of 2195 Al-Li alloy in neutral NaCl solution. It is found that T_1 acts as the main anodic phase during the initial stage of corrosion. At the later stage, the potential of T_1 moves to a positive direction and becomes cathodic to the adjacent alloy base, due to the preferential dissolution of Li from T_1. It is suggested that the association of corrosion with T_1 is caused by the alternate anodic dissolution of T_1 and its adjacent alloy base, which accelerates the corrosion of the alloy base

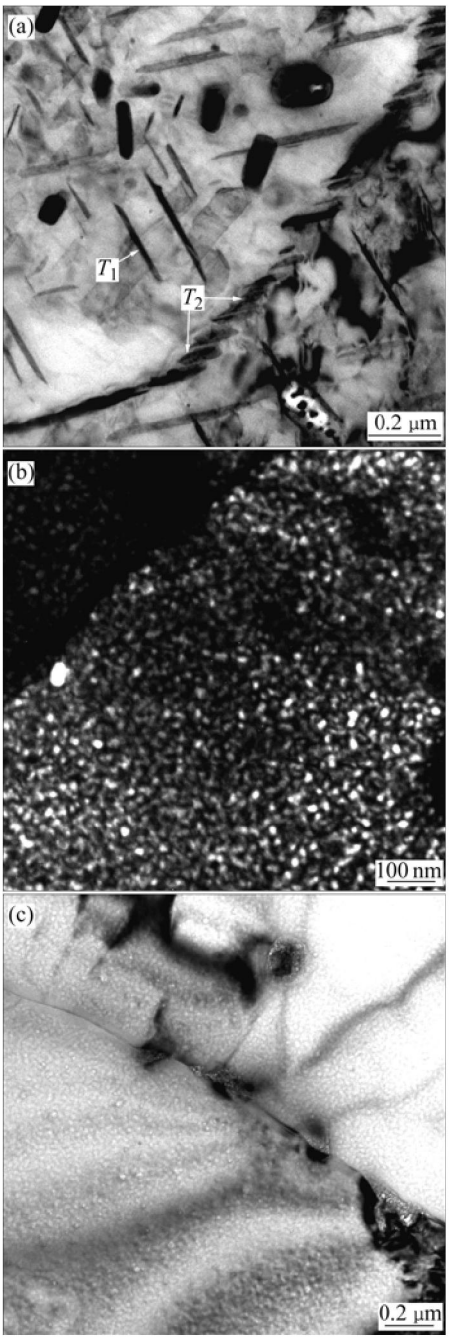

Fig.9 TEM micrographs of peak-aged 2195 and 1420 Al-Li alloys: (a) 2195 alloy, bright field; (b) 1420 alloy, black field; (c) 1420 alloy, bright field

[14,15]. To illustrate the corrosion mechanism associated with T_2, a 2195 Al-Li alloy was aged at a high temperature of 300 ℃ for a long time of 24 h, and its TEM sample was immersed in NaCl solution for 1 h and observed with a Tecnai G^2 TEM. It is found that T_2 is attacked and no corrosion occurs at the adjacent PFZ during the initial stage of immersion, as seen in Fig.10. Due to the distribution of T_2 at grain boundaries and PFZ at its adjacent periphery, 2195 Al-Li alloy is susceptible

to intergranular corrosion. While the distribution of T_1 within grains accelerates the corrosion of alloy base.

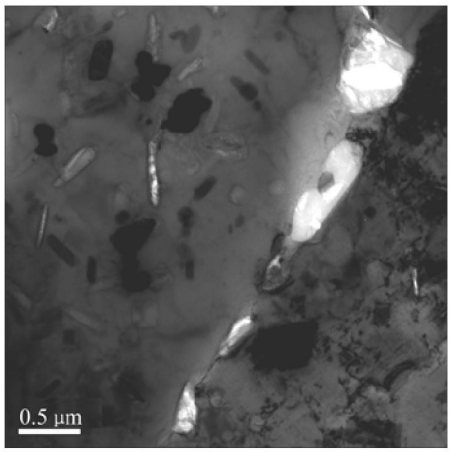

Fig.10 TEM micrograph of 2195 alloy immersed in NaCl solution for 1 h

4.2 EIS analysis

It is well known that EIS reflects the surface structure of the corroded alloy. At the initial stage, only the original flat surface causes a capacitive arc in the EIS plot. As immersion time is increased, localized corrosion, such as pitting corrosion and intergranular corrosion occurs, resulting in that the alloy surface is divided into two parts. One is a flat surface, on which the general corrosion occurs. The other is a new surface caused by localized corrosion. The two capacitive arcs in the EIS at the later stage should correspond to these two parts of the alloy surface. The capacitive arc at the high frequency is caused by the flat surface and that at low frequency corresponds to the new surface[15].

According to this attacked surface structure, the equivalent circuit model is designed, as shown in Fig.11. In this equivalent circuit, R_s is the electrolyte resistance, which could be negligible. The capacitance corresponding to the flat surface is represented by C_1. The charge-transfer resistance and the capacitance corresponding to the new surface are described as R_t and C_2 respectively, while R_p is the resistance through the pore.

A better simulation between the model and the experimental data could be obtained if the capacitance in this circuit is replaced with a constant-phase element (CPE), which is defined by the following equation:

$$Z_{CPE} = Z_0/(j\omega)^{\alpha}$$

or

$$Y_{CEP} = 1/Y_0 \cdot (j\omega)^{\alpha}$$

where Z_0 (or Y_0) and α are constants, ω is angular frequency, and $j=\sqrt{-1}$. For $\alpha=1$, Z_{CPE} represents an ideal capacitance; $\alpha=0$, a resistance; $\alpha=-1$, an inductance; and $\alpha=0.5$, a Warburg impedance.

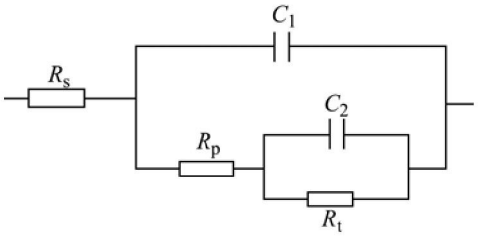

Fig.11 Equivalent circuit used for this study

Figs.12 and 13 display the simulated parameter values for various immersion times. It is found that the values of simulated C_1 and C_2 of the stressed 1420 Al-Li alloy are greater than those of the stressed 2195 AL-Li alloy, which should be explained by surface difference between the attacked 1420 alloy and 2195 alloy. It is observed that no general corrosion and only pitting corrosion with slight corrosion cracks occur on the stressed 1420 Al-Li alloy (in Fig.6), while severe general corrosion and localized corrosion occur on the stressed 2195 Al-Li alloy (in Fig.7(b) and Fig.8(b)). As a sequence, larger flat surface and thinner corrosion film of the stressed 1420 Al-Li alloy raise C_1 value. Although

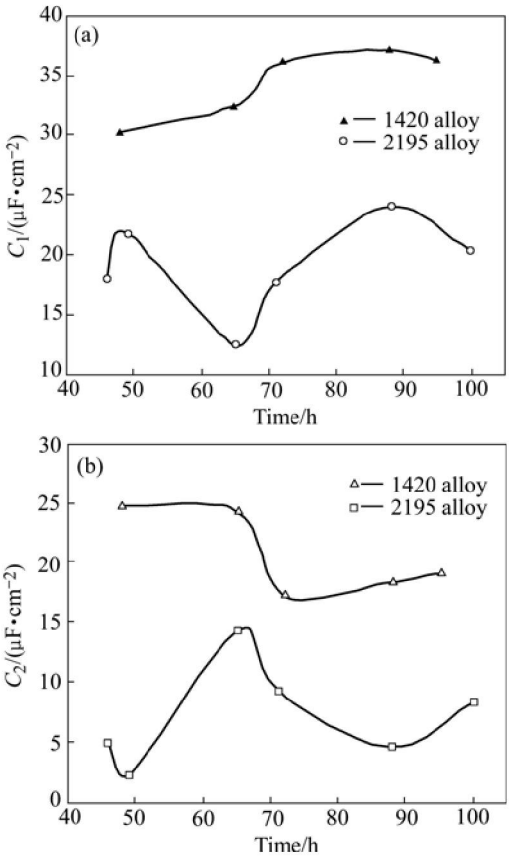

Fig.12 Simulated parameters of C_1 (a) and C_2 (b) for stressed 1420 and 2195 Al-Li alloys

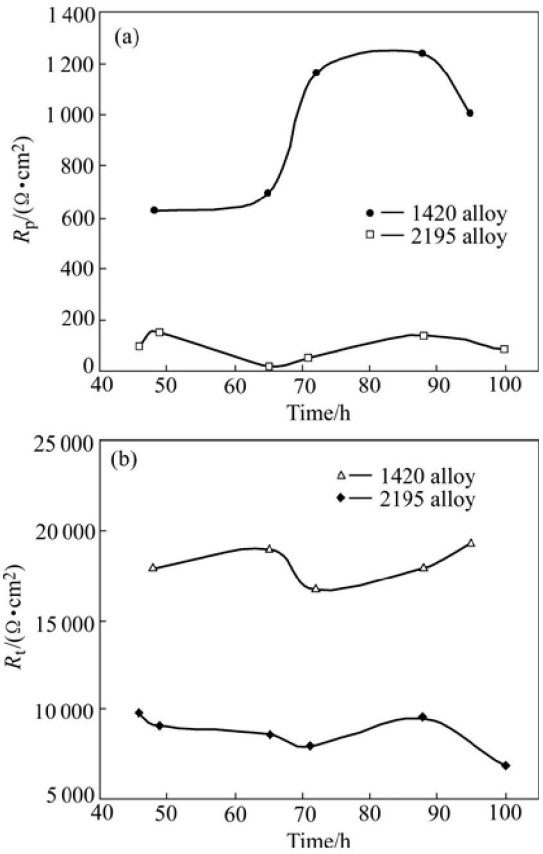

Fig.13 Simulated parameters of R_p (a) and R_t (b) for stressed 1420 and 2195 Al-Li alloys

the new surface of the stressed 2195 Al-Li alloy caused by severe localized corrosion is much greater than that of the stressed 1420 Al-Li alloy, its C_2 value is less than that of the stressed 1420 Al-Li alloy, due to the thick corrosion product on the new surface, as seen in Fig.12(b).

It is found that R_p of the stressed 2195 Al-Li alloy is less than that of the stressed 1420 Al-Li alloy, which is the reflection of a lager localized corrosion size of the stressed 2195 Al-Li alloy. Once localized corrosion, such as intergranular corrosion occurs on 2195 Al-Li alloy, it is easy to penetrate to the inside due to the distribution of T_2 at grain boundaries, indicated by its lower charge-transfer resistance R_t.

5 Conclusions

1) The unstressed 1420 Al-Li alloy in 3.5% NaCl solution is featured with large and discrete pits, while general corrosion and localized corrosion including intergranular corrosion and pitting corrosion occur on the unstressed 2195 alloy.

2) As a tensile stress of 308 MPa is applied to 1420 Al-Li alloy, the pit becomes denser and its size is decreased. While, in 2195 Al-Li alloy under tensile stress of 490 MPa, intergranular corrosion is aggravated and severe general corrosion is developed from connected pits.

3) The EIS analysis shows that more severe general corrosion and localized corrosion occur on the stressed 2195 Al-Li alloy than on 1420 Al-Li alloy. It is suggested that the tensile stress has a greater effect on the corrosion of 2195 Al-Li alloy than on 1420 Al-Li alloy.

References

[1] XIA De-shun. Technological research of tank structural material for launch vehicle [J]. Missles and Sapce Vehicles, 1999(3): 32−41. (in Chinese) .

[2] LIU Xiao-dong, FRANKEL G S, ZOOFAN B, ROKHLIN S I. Effect of applied tensile stress on intergranular corrosion of AA2024-T3 [J]. Corrosion Science, 2004, 46: 405−4250

[3] LI Jin-feng, ZHANG Zhao, ZHENG Ziqiao, TAN Cheng-yu, ZHANG Jian-qing. Influence of tensile stress on exfoliation corrosion and electrochemical impedance spectroscopy of 7075 Al alloy [J]. Corrosion Science and Protection Technology, 2005, 17(2): 79−82. (in Chinese)

[4] ZHANG Z, CAI C, CAO F H, GAO Z N, ZHANG J Q, CAO C N. Evolution of the electrochemical characteristics during pitting corrosion of pure aluminum in sodium chloride solution [J]. Acta Metallurgica Sinica, 2005, 4(18): 525−532.

[5] CAO F H, ZHANG Z, SU J X, ZHANG I Q. Electrochemical impedance spectroscopy analysis on aluminum alloys in EXCO solution [J]. Materials and Corrosion, 2005, 56(5): 318−324.

[6] CHENG Y L, ZHANG Z, CAO F H, LI J F, ZHANG J Q, WANG J M, CAO C N. A study of the corrosion of aluminum alloy 2024-T3 under thin electrolyte layers [J]. Corrosion Science, 2004, 46(7): 1649−1667.

[7] LI Jin-feng, ZHANG Zhao, CAO Fa-he, CHENG Ying-liang, ZHANG Jian-qing, CAO Chu-nan. Investigation of exfoliation corrosion of rolled 8090 Al-Li alloy using electrochemical impedance spectroscopy [J]. Trans Nonferrous Met Soc China, 2003, 13(2): 320−324.

[8] CONDE A, DE DAMBORENEA J. Evaluation of exfoliation susceptibility by means of the electrochemical spectroscopy [J]. Corrosion Science, 2000, 42(8): 1363−1377.

[9] BONORA P L, ANDREI M, ELIEZER A, GUTMAN E M. Corrosion behavior of stressed magnesium alloys [J]. Corrosion Science, 2002, 44(4): 729−749.

[10] KUMAR K S, BROWN S A, PICKENS J R. Microstructure evolution during aging of an Al-Cu-Li-Ag-Mg-Zr alloy [J]. Acta Mater, 1996, 44(5): 1899−1915.

[11] NISKANEN P, SANDERS T H, KINKER J G. Corrosion of aluminum alloys containing lithium [J]. Corrosion Science, 1982, 22(4): 283−304.

[12] WEI Xiu-yu, TAN Cheng-yu, ZHENG Zi-qiao, LI Jin-feng, LI Hai, LI Yan-fen. Influence of aging on corrosion behavior of 2195 Al-Li alloy [J]. The Chinese Journal of Nonferrous Metals, 2004, 14(7): 1195−1200. (in Chinese)

[13] MURKEN J, HOHNER R, STROTZKI B. Strain path dependence of the precipitate size evolution of an Al-Mg-Li alloy under combined thermal and mechanical loading [J]. Materials Science and Engineering A, 2003, 363(1−2): 159−170.

[14] LI J F, ZHENG Z Q, JIANG N, LI S C. Study on localized corrosion mechanism of 2195 Al-Li alloy in 4.0% NaCl solution (pH6.5) using a three-electrode coupling system [J]. Materials and Corrosion, 2005, 56(3): 192−196.

[15] CONDE A, DE DAMBORENEA J. Electrochemical modeling of exfoliation corrosion behavior of 8090 alloy [J]. Electrocimica Acta, 1997, 43(8): 849−860.

(Edited by YANG Bing)